Development 116, 11-20 (1992)
Printed in Great Britain © The Company of Biologists Limited 1992

Development of the *D. melanogaster* caudal segments involves suppression of the ventral regions of A8, A9 and A10

D. T. KUHN[1*], M. SAWYER[1], G. PACKERT[1], G. TURENCHALK[1], J. A. MACK[1], TH. E. SPREY[2], E. GUSTAVSON[3] and T. B. KORNBERG[3]

[1]*Department of Biology, University of Central Florida, Orlando, Florida 32816, USA*
[2]*Department of Biology, University of Leiden, 2300 RA Leiden, The Netherlands*
[3]*Department of Biochemistry and Biophysics, University of California, San Francisco, California 94143, USA*

*Author for correspondence

Summary

Whereas the segmental organization of the thorax and anterior abdomen is morphologically delineated in both the *Drosophila* larva and adult, segments in the head and caudal regions lack such well-defined boundaries. Consequently, the organization of these regions has been difficult to decipher. In this study, transformations caused by the bithorax-complex homeotic mutants *48, M3, Ultraabdominal-1* (*Uab[1]*) and *tumorous-head-3* (*tuh-3*), as well as the patterns of *engrailed* gene expression have been analyzed to investigate the segmental organization of the caudal segments. A special emphasis was placed on sense organs appearing in abdominal segments 8, 9 and 10 (A8-A10): We find that: (1) transformations in the caudal segments obey parasegmental borders; (2) the sense organs on A8, A9, and A10 are probably homologous to the pits and hairs in anterior A1-A7; (3) except for the larval anal tuft and the anterior side of A8, all structures in larval segments A8, A9 and A10 are dorsal/lateral in origin; and (4) dorsalization of embryonic A8 and A9 cells leaves space ventrally for A10, as it follows the contracting ventral nervous system during the embryological process of germ band contraction.

Key words: *Drosophila*, larval cuticle, homeotic mutants, parasegments, sense organs.

Introduction

The body plan for *D. melanogaster* is set by four classes of genes. The earliest-acting are maternal effect genes which establish polarity and spatial coordinates of the egg and developing embryo (Nusslein-Volhard, 1979). After zygote formation, products of maternal effect genes interact with gap genes and segmentation genes or their products to establish the number and spatial organization of the segments (Nusslein-Volhard and Wieschaus, 1980; reviewed by Akam, 1987). A fourth class of genes, the homeotics, then provide an identity to each segment (Duncan, 1987). Most homeotic genes act in parasegments (PS), metameric units composed of the posterior compartment of one segment *(P)* together with the anterior compartment *(A)* of the adjacent segment (reviewed by Martinez-Arias and Lawrence, 1985).

Most insects have eleven abdominal segments (A1-A11) with a non-segmental telson at the posterior end (see review by Matsuda, 1976). However, the number of segments in most holometabolous insects is reduced. *Drosophila*, for example, has eight recognizable abdominal segments as well as caudal regions of uncertain identity. Segments posterior to A8 have either disappeared through the course of evolution, fused with each other and/or with A8, or have been lost due to a combination of fusion and partial suppression. This complex developmental program of creation/fusion/suppression, with the absence of any morphological manifestation of segmental boundaries in this region, and the paucity of easily-scored cuticular specializations, obscures the organization of the caudal end.

Several previous studies have addressed the question of the number and identity of the caudal segments of *Drosophila.* Although investigators appear to agree that there are at least ten abdominal segments, there is no consensus as to which parts (compartments) of each segment are present. Jürgens fate-mapped caudal structures of the 1st instar larval cuticle to the blastoderm using ultraviolet laser ablations and analyzed cuticular phenotypes of mutant embryo/1st instar larvae (Jürgens, 1987). Although the precision of this analysis was severely limited by the paucity of structures, he concluded that segments A8 and A10 contain both *A* and *P* compartments, but that A9 has only an *A* compartment. Patterns of sensory neurons in embryos suggest that A8 has both *A* and *P* compartments, but provide no evidence for *P* compartments in A9, A10, or A11

(Hartenstein, 1987). Lastly, the lack of early clonal restrictions in adult genitalia and the requirement for *engrailed* function in the genital disc was interpreted to indicate that the *A* compartments of A8 through A10 may be either suppressed or missing, leaving only *P* compartments to differentiate all genital structures (Janning et al., 1983).

Development of the genitalia and of the caudal segments is controlled by the homeotic genes in the bithorax-complex (BX-C; Lewis, 1978). The BX-C has three major genes, *Ubx*, *abd-A* and *Abd-B* (Sanchez-Herrero et al., 1985; Tiong et al., 1985; Casanova et al., 1986) which together provide identities to the segments from the posterior side of thoracic segment 2 (pT2), thoracic segment 3 (aT3 and pT3), all abdominal segments, and the genitalia (Lewis, 1978). *Ubx* regulates the development of pT2-aA1, *abd-A* regulates the development of pA1-aA8, and *Abd-B* regulates the development of pA4-A10 (reviewed by Duncan 1987; this study). *Abd-B* has been subdivided into a proximal (*m*) morphogenetic function and a distal regulatory (*r*) function, based upon complementation analysis (Casanova et al., 1986). At the molecular level, *m* function is encoded by the class A transcript, while *r* function is encoded by the class B and class C transcripts (Boulet et al., 1991). Mutants affecting individual abdominal segments are referred to as *infra-abdominal* (*iab*; Lewis, 1978), and are alleles of *abd-A* and *Abd-B.* Each *iab* mutant is designated by the anterior compartment of the segment most affected (Duncan, 1987). Typically, an *iab* mutant transforms an abdominal segment (or parasegment) into a more anterior neighbor. In this study, such homeotic transformations were analyzed in *Abd-B* mutants affecting *m* function (*M3* and *48*) and *r* function (48, *Uab*^{1} and *tuh-3*.)

Since segmentation of the *Drosophila* embryo takes place by the cellular blastoderm stage, and since the distinct larval and adult forms derive from the cellular blastoderm following the complex movements of gastrulation, germ band extension, germ band retraction and dorsal closure, understanding the segmental organization of the different stages requires that the identity of the different parts be determined for each stage. Moreover, since the first instar larval cuticle and the adult cuticle develop independently - the former by the polyploid larval epidermis, and the latter by the diploid imaginal cells that replace the larval cells during metamorphosis - the relationship of the embryonic segments to the larval and to the adult structures must be determined separately. This has not been possible for the caudal segments, and considerable uncertainty about their organization persists.

This is a study of the segmental organization of the larval caudal region. We have analyzed the large, more complex, and more easily scored structures of the third instar larva. Since the epithelial cells which secrete the larval cuticle do not move during the larval molts, the overall cuticular organization of the three larval instars does not change, and the patterns of the different larval stages can be compared directly. We first obtained a more detailed description of the cuticle morphology of the third instar larval skin. We then followed the expression of *engrailed* in both embryos and third-instar larvae to track the anterior and posterior compartments from the cellular blastoderm through to the fully-formed larval cuticle. For this study we assume that all cells expressing *engrailed* belong to posterior compartments and that cells not expressing *engrailed* are anterior only. Finally, we related these patterns to the cuticle patterns of both normal and homeotically transformed larvae. We find that maturation of the caudal segments involves both suppression and fusion of segmental primordia, and that complex movements during embryogenesis lead to a positional reorganization of A8, A9 and A10.

Materials and methods

Drosophila stocks used

(1) Canton-S. A wild-type laboratory strain (Lindsley and Grell, 1968). (2) Uab^{1}/TM6B, Tb. Uab^{1} is an *r* mutant associated with a tiny inversion in the bithorax-complex (BX-C) with one breakpoint in the bithoraxoid (bxd) region and the second in the posterior *Abd-B* region at +185 kb on the DNA map (Fig. 1) (Karch et al., 1985; Duncan 1987). TM6B, Tb is a third chromosome balancer chromosome carrying the dominant larval marker *Tubby (Tb*). Homozygosity for *Uab*^{1} results in a strong loss of function *bxd* phenotype and a loss of external and internal genitalia due to the *r* lesion. The dominant gain of function *Uab*^{1} phenotype in heterozygotes results in transformation of abdominal segment 1 (A1) into abdominal segment 2 (A2) (Kiger, 1976). (3) *tuh-1*^{g}; *tuh-3*. Homozygosity for the wild-type maternal effect allele *tumorous-head-1*^{g} *(tuh-1*^{g}), located in the base of the X-chromosome, causes the *r* mutant *tumorous-head-3 (tuh-3*) to act as a recessive mutant, resulting in a loss of genitalia (Kuhn et al., 1981). *tuh-3* likely resulted from the insertion of the mobile element Delta-88 at +200 kb on the DNA map (Karch et al., 1985; Fig. 1). (4) *M3*. *M3* is an EMS induced *m* mutant (Sanchez-Herrero et al., 1985) which has not been mapped to the DNA level. (5) *48*. *48* is a mutant with impaired *m* and *r* function associated with inversion In(89E-100C) (Celniker et al., 1990). The BX-C breakpoint is between +159 to 162 kb (Celniker et al., 1990; J. A. Mack, unpublished data; Fig. 1). (6) *ryXho25*. *en*$^{+}$ *lacZ* is a transformed strain in which the *E. coli* β-galactosidase gene expresses β-galactosidase under the control of the *engrailed* promoter in all posterior compartments (Hama *et al.*, 1990). (7) *Df (3R) P9/Sb, Dp (3;3) P5*. *Df-P9* is a deficiency for the entire BX-C, balanced by a duplication for the complex.

Stock maintenance

All *Drosophila* stocks were maintained at room temperature, approximately 24°C, on a standard medium consisting of cornmeal, agar, dried yeast extract, dextrose, sucrose, propionic acid and phosphoric acid. Tegosept was added to the surface of the medium to suppress mold growth.

Preparation of larval epidermis

Larval cuticles were prepared for microscopy following a modification of the procedure of Van der Meer (1977). Larvae were cleared in Nesbitt's fluid for up to 1½ hours and small holes poked in them with a sharp tungsten needle. Larvae were then transferred to a microscope slide in a drop of Hoyer's solution and placed under a coverslip or were cut laterally, opened up and flattened in a drop of Hoyer's and prepared as previously described. Identification and segmental and parasegmental identity of the caudal cuticular structures relies on the published results of Sato and Denell (1986), Whittle et al. (1986), Jürgens (1987) and Turner and Mahowald (1979) and our studies of the 1st and 2nd instar larvae (Kuhn et al., 1992).

Staining for β-galactosidase

The procedure used to stain for β-gal activity was similar to that

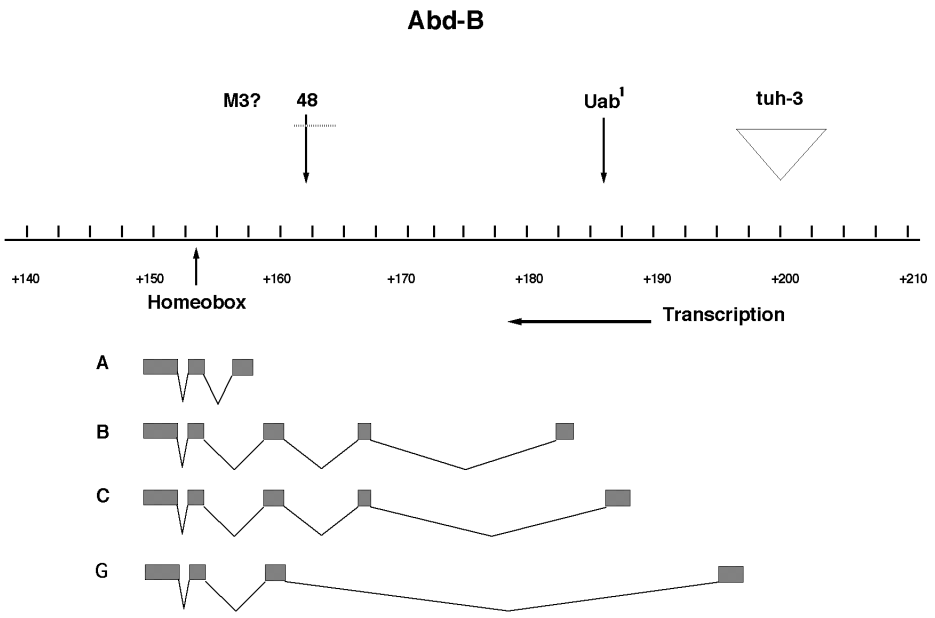

Fig. 1. Partial DNA map of the BX-C *Abd-B* gene is shown with locations of homeotic mutants used in this study (adapted from Karch et al., 1985). The location of the *M3* lesion has not been identified. The suggested *M3* region is inferred from developmental/genetic data. Below the DNA line are the *Abd-B* transcripts adapted from (Boulet et al., 1991).

used by Hama et al. (1990). Our procedure differed in that 3rd instar larvae were injected directly with phosphate-buffered saline (PBS) + 2% EM grade glutaraldehyde to fix the tissue and to balloon the larva. The posterior spiracles are forced to fully extend as are the larval sense cones, while the larval muscles become brittle and break. After fixation for 2-20 minutes, the larvae were cut laterally in PBS, washed for 2-5 minutes in PBS and then placed in the staining solution (Hama *et al.*, 1990) overnight or until the staining pattern fully developed. Larvae were permanently mounted on slides in Faure's for analysis and photography.

Immunological detection of the en$^+$ protein

The *engrailed (en$^+$)* expression in embryos was revealed by staining wild-type embryos with anti-engrailed antiserum as described by Karr et al. (1989).

Results

Morphology of the caudal region of the 3rd instar larva

While the cuticle patterns of the 1st instar larva, particularly the caudal end, have been thoroughly analyzed (Turner and Mahowald, 1979; Lohs-Schardin et al., 1979; Whittle et al., 1986; Sato and Denell, 1986; Jürgens, 1987), cuticle patterns of the 2nd and 3rd instar stages have received less attention (Hertweck, 1931; Dambly-Chaudiere and Ghysen, 1986; Kankel et al., 1980). The 3rd instar larva is considerably larger than the 1st instar larva, and its cuticular features are both larger and easier to detect and characterize. To establish the wild-type pattern of cuticular specializations on the caudal segments of the 3rd instar larva, approximately 20 wild-type Canton-S larvae were examined in detail. A summary view (with some features enhanced for better viewing and some minor features omitted) is provided in Fig. 2.

Dorsal and lateral surfaces

Whereas the dorsal surface of the 1st instar larva is blanketed with hairs, the dorsal surface of the 2nd and 3rd instars is not. The hairs in later instars are replaced by larger spinules, which, unlike the ventral denticles, are not pigmented. Abdominal segments A1-A7 have a stripe of naked cuticle posterior to the spinule band. This stripe has a characteristic assemblage of pits and hairs (see Dambly-Chaudiere and Ghysen, 1986). In contrast, dorsal aA8 has many spinules in the homologous position and has no naked cuticle stripe. As described by Jürgens (1987), the posterior border of A6 is marked by the most posterior row of anterior-pointing spinules, and the 1st posterior-pointing spinule row marks the anterior side of A7. The lateral portion of A7 also has a band of spinules and a naked stripe with several specialized pits and hairs.

Ventral surface

Prominent denticle belts mark the ventral surface (Fig. 2). In A1-A7, these belts overlap the segment borders: the first two rows of each belt point anteriorly and are in the posterior compartment, whereas the next most posterior rows point posteriorly and are in the anterior compartment of the adjacent segment. One anterior-directed and two posterior-directed denticle rows complete these belts. Within each segment is a stripe of naked cuticle with specialized abdominal pits. aA8 lacks the most posterior denticle rows and the stripe of naked cuticle.

Caudal sense organs

Seven prominent sense organs (SOs) are located in the region posterior to A7 (Fig. 2). We identify them using the nomenclature of Whittle et al. (1986) and Sato and Denell (1986). Their structure in the 1st instar larva has been described (Sato and Denell, 1986), and although they retain the same relative position with each larval molt, their morphology changes (Kuhn et al., 1992). Basically, there are two types of SOs. SO3, SO5 and SO7 have pegs on their apex in all instar stages. In contrast, SOs 1, 2, 4 and 6, which have a hair sensillum in the 1st instar larva (Fig. 3A), have a more complex structure with a central knob surrounding broad based spinules in the 2nd instar. Depending upon the SO, the number of apposing spinules may be

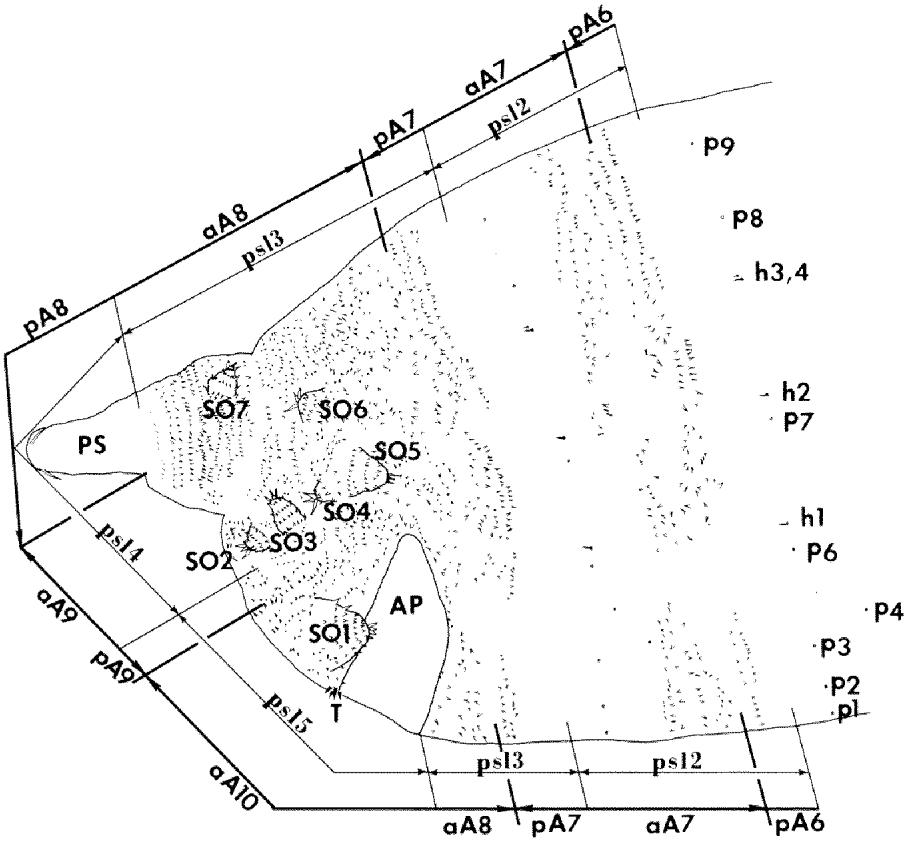

Fig. 2. Camera lucida drawing of the caudal segments of a Canton-S 3rd instar larva. This lateral view is positioned with dorsal side up. Abdominal pits and hairs are common from A1-A7. Sense organ SO1 is located in aA10, SO2-SO4 are in aA9, while SO5-SO7 are located in aA8. General locations of segment and parasegment borders are given. AP, anal pad; aA1-aA10, anterior compartments of abdominal segments 7 through 10; h1-h4, abdominal hairs 1 through 4; p1-p9, abdominal pits 1 through 9; PS, posterior spiracles; SO1-SO7, sense organs 1 through 7; T, tuft.

3, 4 or 5. In the 3rd instar, these SOs have apposing leaflet shaped structures (Fig. 3B, C).

Posterior compartments in the caudal region of the embryo

The *en*$^{+}$ protein present at various stages of embryogenesis was detected with a monoclonal antibody directed against an epitope in the *engrailed* homeodomain (Patel et al., 1989). In early gastrulas, engrailed protein is present in stripes that alternate in intensity (Fig. 4A). By embryonic stages 9-10, 9 stripes of engrailed protein are present in the abdominal segments, including ones in pA8 and pA9 (Fig. 4B). Embryos beginning germ band retraction have a narrow but complete band of pA9 stained cells and a fully developed pA8 band (Fig. 4C). At this stage, the anus is forming at the ventral midline in what appears to be aA10; this region is unstained. Out of focus in Fig. 4C, but clearly visible in Fig. 4D, is the hindgut; it is partially stained. The position of the stained hindgut is consistent with an identity of pA10.

As the germ band retracts, the cells of pA9 and pA8 pull away from the ventral nervous system and migrate dorsally (Fig. 4E through 4J). The aA10 anal region, anus and presumptive anal pads, and hindgut then follow the ventral nervous system around the end of the embryo as it contracts (Fig. 4E through 4H).

The shape of the pA8 cell groups changes gradually during germ band retraction from straight lines (Fig. 4D) to irregular triangles (Fig. 4E, F), to "v" shaped bands (Fig. 4G, H), and finally to complete rings (Fig. 4I). Throughout germ band retraction the two groups of pA8 cells migrate dorsally, eventually fusing at the dorsal midline (Fig. 4J). The fused pA8 circles are within the base of the posterior spiracles (Fig. 4L). In some preparations (not shown here), stained cells were also present on the lateral sides of pA8, suggesting the existence of small lateral pA8 cell groups as well, but no other vestige of ventral pA8 was evident after germ band retraction. The two groups of pA9 cells migrate dorsally around the presumptive anus/anal pad, eventually fusing at the dorsal midline at the distal tip of the embryo (Fig. 4E-J). This cellular migration provides the anal region with a ventral position beneath A8 and A9. At no stage was engrailed protein detected in a region that would suggest the existence of a pA11 compartment.

Engrailed and engrailed-lac Z expression in older embryos

Fig. 5 shows the transition in staining in late embryos to the pattern found in the 1st larval instar stage and subsequent larval stages. The germ band-retracted stage-12 embryo shown in Fig. 5A shows the ventral epidermis as a sheet of transparent tissue covering the ventral nervous system, with narrow engrailed stained stripes. The most posterior ventral engrailed stained strip encircling this embryo belongs to pA7. A small group of lateral pA8 stained cells are visible. All pA9 cells belong to a band of cells situated dorsal to the anal pad. We have not seen the lateral pA8 stained band extend further than seen here or in Fig. 5B. By embryonic stage 14-15, engrailed stain is significantly reduced in the epidermal stripes (Fig. 5B). This *ryXho25* embryo has been double stained for engrailed and β-galactosidase. Note the pattern is the same as seen in Fig. 5A. The small band of pA8 cells remain lateral. This feature is retained through the 3rd instar stage, as shown later

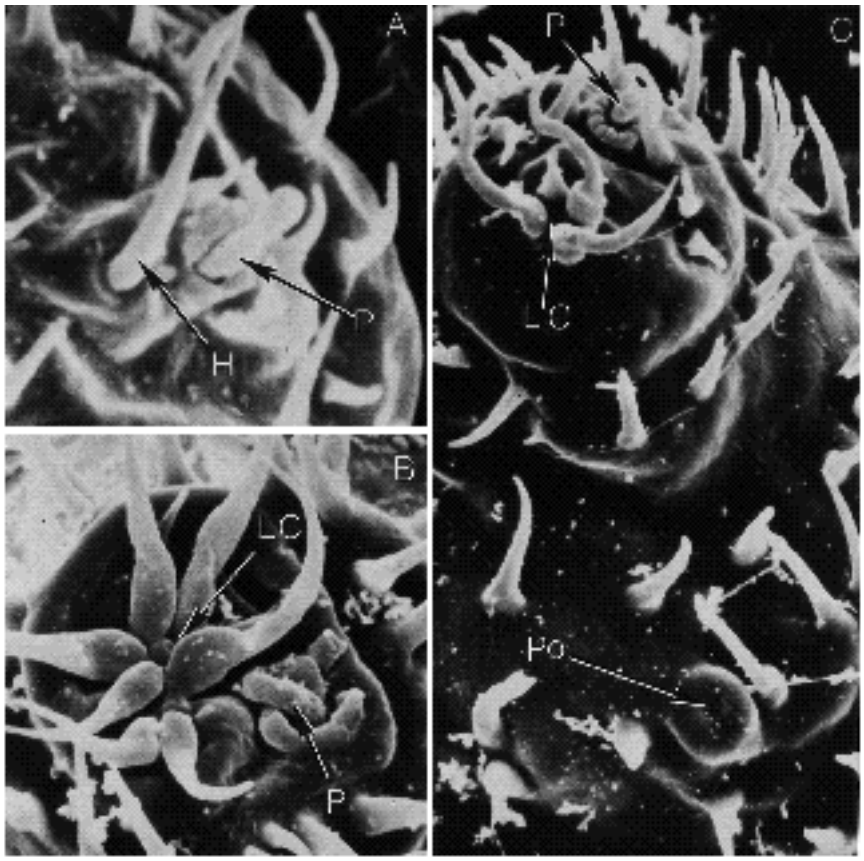

Fig. 3. SEM photomicrographs of caudal sense organs. (A) Apex of a 1st instar SO2 that possesses a peg and hair sensillum, ×4000. (B) Apex of a 3rd instar SO2 that possesses a peg and a structure with a central knob surrounded by broad based apposing leaflets, ×2500. (C) Apex of a 3rd instar SO1 containing a peg and leaflet structure, plus a pore or campaniform sensilla in the SO1 base. H, hair; LC, leaflet cluster; P, peg; Po, pore.

in Fig. 7B. The engrailed stained stage-15-16 embryo shown in Fig. 5C has engrailed stained cells filling the posterior spiracles and has the stained band of pA9 cells. The darkly stained ventral nervous system is covered by the transparent sheet of cells now almost devoid of engrailed stain. The *ryXho25* β-galactosidase stained embryo in Fig. 5D was close to hatching as a 1st instar larva. Out of focus is the cuticle with hairs and denticles that had formed. This stage-17 embryo has the same staining pattern as seen in Fig. 5A-5C. It shows the typical pA8 stained cells in the spiracles, which persist through the 3rd instar stage as shown later in Fig. 7A. The same is true for all other components of the pattern, including the pA9 and pA7 bands, as also seen in the 3rd instar larva featured Fig. 7A.

Posterior compartments in the caudal region of the 3rd instar larva

Since engrailed protein in larval epidermal cells is difficult to detect with immunohistochemical probes, posterior compartment cells in the cuticle of 3rd instar larvae were mapped with a transgenic fly strain that expresses β-galactosidase under the control of the *engrailed* promoter. In cuticle preparations from this strain, β-galactosidase activity is robust and identifies posterior compartment cells (Hama et al., 1990). The *lac Z* stained cells are assumed both to stain posterior compartment cells only and to stain the same cells recognized by the engrailed monoclonal antibody. To study the organization of the caudal region of 3rd instar larvae, we compared both the cuticle morphology and the distribution of β-galactosidase-containing cells in normal and mutant 3rd instar larvae.

Dorsolateral views of the caudal end with a SEM reveal the prominent sense organs SO1 through SO5 and, partially obscured, sense organs SO6 and SO7 (Fig. 6A). β-galactosdiase activity localizes to three areas in this region (Figs 6B, 7A,B). One area is the distal portion of fully extended posterior spiracles, consistent with a pA8 designation (see previous section). At the ventral base of the posterior spiracles are paired stretch receptors which also contain β-galactosidase (Figs 6B, 7A). Since stretch receptors extend from lateral posterior compartments into anterior compartments in all larval abdominal segments (Hama et al., 1990), we propose that the unstained region ventral to pA8 spiracles (which includes SO2, SO3 and SO4) is aA9. A second area with β-galactosidase activity consists of a narrow band of about 11 cells between SO4 and SO5 (Figs 6B, 7A,B). The dependence of this stained area on *r* function (see below) suggests that this band of cells is part of pA8. The third area is near the anal pad (Figs 6B, 7A), and is in the appropriate position to be pA9 (see Fig. 3 and homeotic data below). A pair of stretch receptors extends from either end of pA9 toward the base of SO3. The location of these stretch receptors suggests that the ends of pA9 originated in the lateral regions of the embryo. If so, then pA9 includes lateral and dorsal but no ventral structures. pA9 also extends anteriorly along the ventral midline and appears to include part or all of the anal tuft. The non-stained area anterior and ventral to pA9 is, based on the observations summarized in Fig. 4, presumed to be aA10. aA10 includes SO1

and the anal pad. Our data do not indicate where derivatives of segment A11 might be located.

This pattern of β-galactosidase activity in the caudal segments of 3rd instar larvae is altered in mutants of the *Abd-B* allele *tuh-3*. *tuh-3* is a loss of function *r* mutant that principally transforms PS14 (pA8/aA9) toward a more anterior segment. In a homozygous *tuh-3* mutant larva carrying the *engrailed-lacZ* transposon, the narrow band of about 11 β-galactosidase-containing cells between SO4 and SO5 expands in two directions: toward the posterior spiracles, and around the rostral side of the anal pad where staining cells extend between the anterior border of the anal pad and the posterior border of the 8th denticle band (Fig. 7C, E; as drawn in Fig. 6D). This pattern contrasts with wild-type larvae, in which no staining cells appear next to the aA8 denticle band, or in or next to SO1 (Figs 6B and 7D). We interpret the altered pattern in the mutant as indicative of a partial transformation of pA8 toward pA7. Expansion of pA8 in mutants to become a continuous band connecting the posterior spiracles with the lateral band (Fig. 7C) and along the anal pad-8th denticle border (Fig. 7E) suggests "a more pA7-like shape". In the wild-type larva, pA7 forms a continuous annulus whereas the ventral portion of pA8 is absent and the lateral and dorsal portions are separated. In addition to these effects on pA8, *tuh-3* causes a reduction in the size of SO4 in aA9, so designated because *tuh-3* transforms PS14 which includes aA9 (Fig. 7G) and because

Fig. 4. Embryos stained for the posterior compartment specific engrailed *(en)* protein are shown. The embryos are ordered to show inversion of A8-A10 during germ band retraction. (A) Alternating dark and light *en* bands of stage 9 or 10 embryo. (B) Germ band-extended embryo with pA9 band in early stage of staining. (C, D) Embryos in early germ band retraction, with hindgut, probably originating from pA10, staining in D. (E - I) Sequence of pictures showing later germ band retraction where pA8 and pA9 split at the ventral midline and the anal region retracts between them. The pA8 and pA9 cell groups migrate dorsally and fuse during dorsal closure. (J) Arrows show single stained cells that appear prior to and after dorsal closure (I-K). (K) Stained cells of the peripheral nervous system are shown. (L) The ring of pA8 cells seen in I and J partially form the posterior spiracles. aA1, aA7, aA10, anterior abdominal segments 1, 7 and 10; an, anus; hg, hindgut; ich5, cells of peripheral nervous system; pA7-pA9, posterior abdominal segments 7 through 9; ps, posterior spiracles; 8vns-9vns, ventral nervous system for A8 and A9.

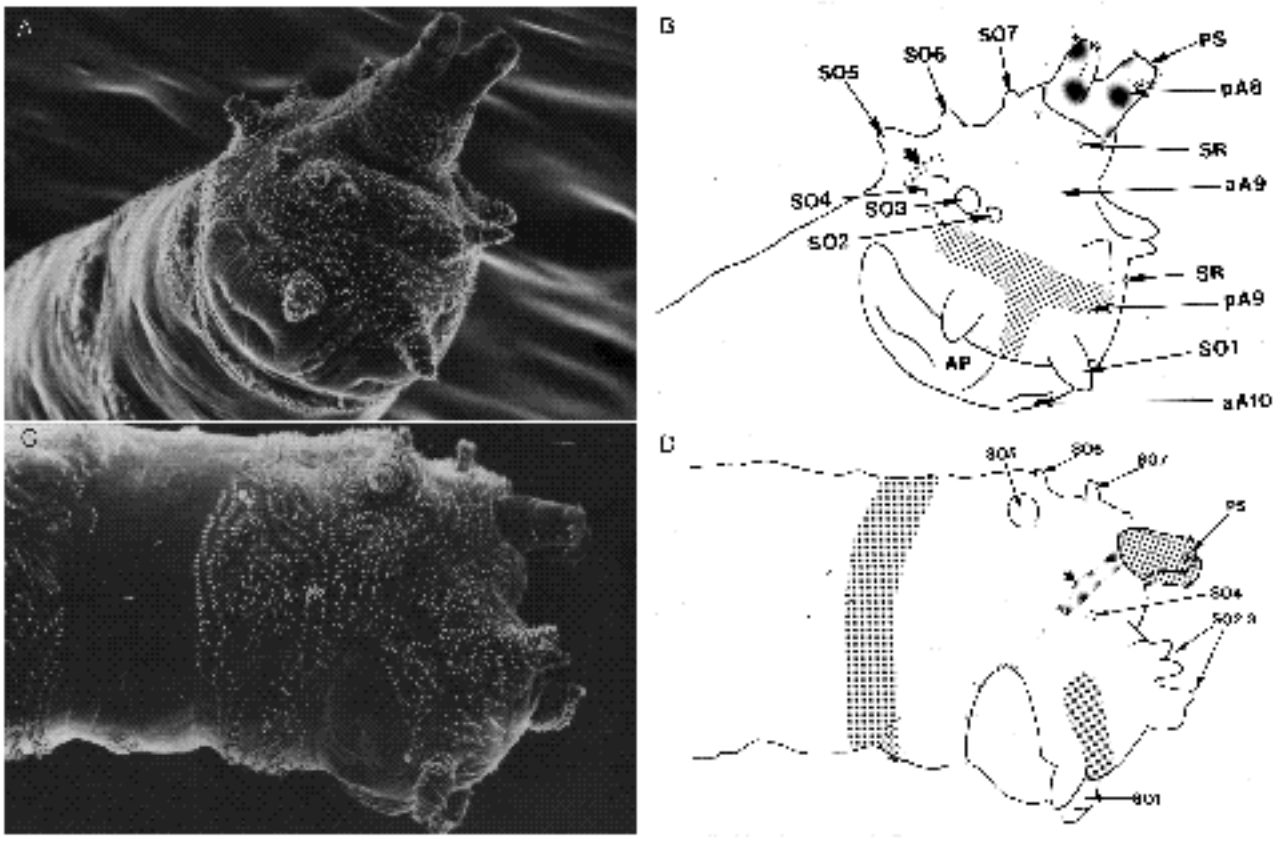

Fig. 6. SEM photomicrographs of wild-type 3rd instar morphology and β-gal distribution and mutant phenotype of *tuh-3*. (A) Ventral aspect of the caudal segments showing the wild-type morphology. (B) Tracing of A with the posterior-compartment-specific β-gal distribution pattern shown by shaded areas. Arrowhead shows small pA8 extension. (C) Lateral aspect of the caudal segments of *tuh-3* transformed 3rd instar larva. (D) Tracing of C showing the β-gal-staining pattern with an enlarged staining zone (arrowhead) between a tiny displaced SO4 and normal SO5 that likely represents an extension of pA8. AP, anal pad; aA9-aA10, anterior compartments of abdominal segments 9 and 10; pA8-pA9, posterior compartments of abdominal segments 8 and 9; PS, posterior spiracles; SO1-SO7, sense organs 1 through 7; SR, stretch receptors.

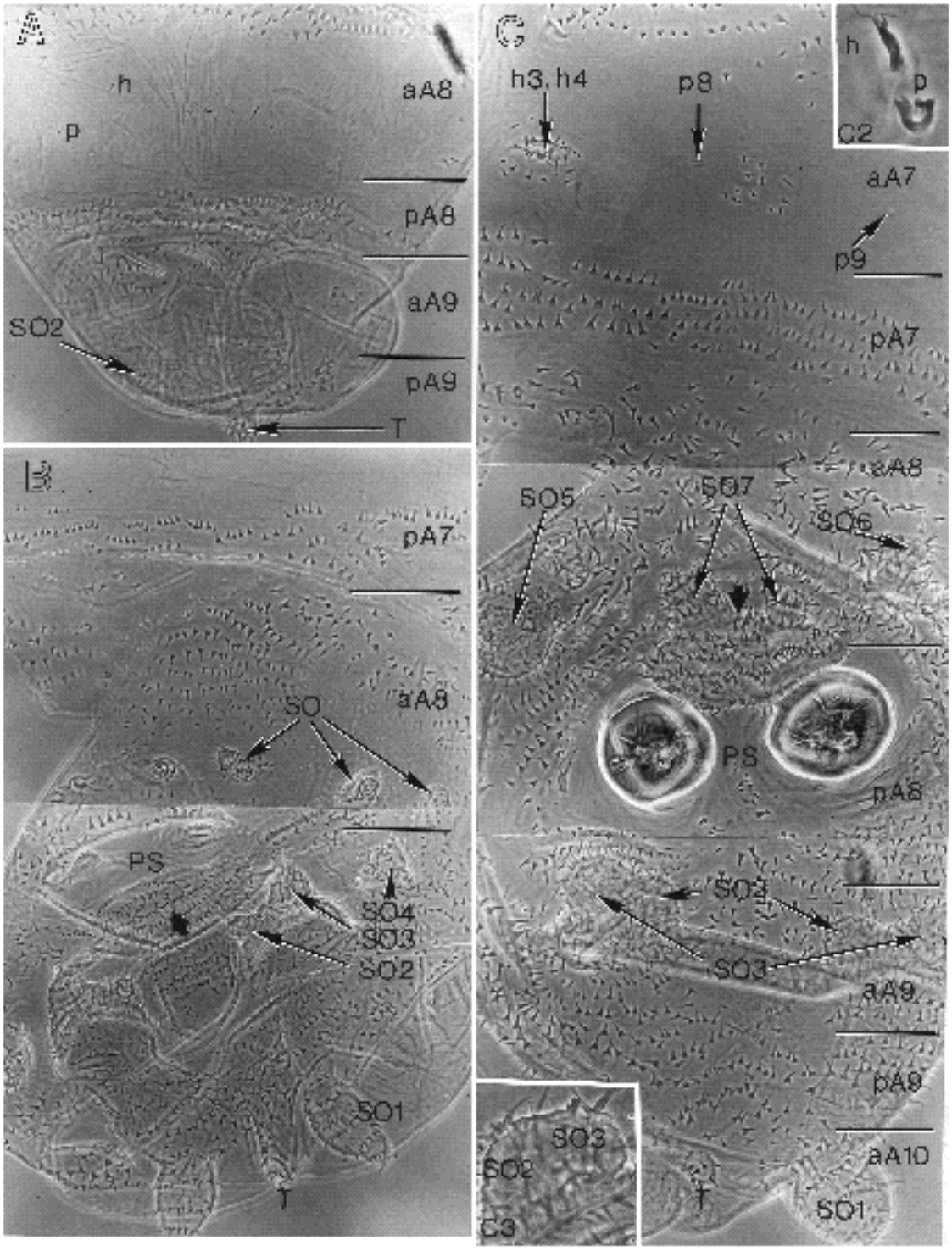

Fig. 8. Phase contrast photomicrographs of homeotic mutant 3rd instar larvae. Location of compartment borders provided for orientation rather than to precisely position borders. (A) Transformations on *48/48* larval abdominal segments 8 and 9. (B) Transformations on *M3/M3* abdominal segments pA7 through SO1 of aA10. Arrowhead identifies spinule patch at base of posterior spiracles. (C) Transformation on Uab^1/Uab^1 larva from aA7 through aA10. Insert C2 in upper right shows peg next to hair in aA7 naked cuticle. Insert C3 at lower left shows fusion of SO2 and SO3. Arrowhead identifies spinule patch at anterior base of posterior spiracles. aA7-aA10, anterior abdominal segments 7 through 10; h3, h4, abdominal hairs 3 and 4; p8, p9, abdominal pits 8 and 9; pA7-pA9, posterior abdominal segments 7 through 9; PS, posterior spiracles; SO1-SO7, sense organs 1 through 7; T, tuft.

SO4 is between the pA8 and pA9 stained regions). *Tuh-3* also causes fusion of SO2 and SO3, but does not affect other sense organs in aA8 or the stained pA9 band (Figs 6C, D and 7G). *tuh-3* also includes a small cluster of spinules around pit p9 in aA7 (Fig. 7H), suggestive of localized gain of function. Note that the pits p8 and p9 are clearly located in the unstained anterior portion of A7 (Fig. 7H).

Homeotic transformations in 3rd instar cuticle

Although studies of cuticular phenotypes of 3rd instar larvae enjoy the advantage of the tremendous growth relative to the tiny 1st instar larva, they are limited in two important ways. Firstly, genetic studies are limited to mutants that survive to the third instar. Secondly, transformations that affect the embryo or larval stages differently become difficult to interpret. Fortunately for our studies, a number of BX-C mutants survive through the 3rd instar stage.

48/48

48/48 3rd instar larvae show a strong loss of *Abd-B* function (Fig. 8A). A large naked cuticle region characteristic of more anterior abdominal segments appears in PS13 (pA7/aA8) (see Fig. 1); SO5, SO6 and SO7 are absent, and in their place, pegs, pits and hairs appear in the naked cuticle region. These changes suggest a transformation of PS13 to a hybrid of PS11 and PS12. Dorsally, there is a slight transformation of PS12 (pA6/aA7) to PS11 (pA5/aA6; not shown), but strong transformations of PS13, PS14 and PS15. An altered spinule region, wide band of naked cuticle, reduction of SO2 to a pit and hair, and SO3 to a peg, again suggest a transformation of PS14(pA8/aA9) to PS12. In PS15 (pA9/aA10), SO1 has only a peg and bifurcated hair (not visible in this plane), indicating a similarly strong transformation.

The ventral effects of the *48* mutation are consistent with this interpretation of the dorsal phenotype. Whereas wild-type 3rd instar larvae have only the denticle band portion of ventral aA8 present (the naked cuticle portion of ventral aA8 and all of pA8 are suppressed), *48* mutants have a region of naked cuticle and a 9th denticle belt, complete with both anterior and posterior pointing denticles (not shown). *48* mutants therefore appear to contain an entire transformed A8. In addition, two additional rows of posterior pointing denticles are present, representing ventral aA9 next to the anal pad. The anal tuft denticles are duplicated (average number 35 denticles vs wild type average of 23 denticles) and in some larvae the anal pad appears distorted.

M3/M3

The dorsal pA7 spinule belt is altered and resembles that of PS11/PS12 (Fig. 8B). The dorsal aA8 spinules are reduced, with more naked cuticle present and with SO5 and SO6 severely reduced in size and aligned across the segment as if they were pits and hairs. In addition, a pad of dorsal spinules is not present on the anterior side of the posterior spiracles where SO7 should be: SO7 appears to have been suppressed (see the wild-type spinule patch identified by the arrow in Fig. 8C). All that remains of the spiracles in M3 are two undifferentiated mounds with oval openings. In some preparations (not shown), a fold of tissue extends from between the transformed spiracles into the naked cuticle region of aA8, perhaps suggesting that portions of the posterior spiracles may be evolutionary modifications to the naked cuticle region. *M3* strongly transforms PS13 (pA7/aA8) toward PS11/PS12, but does not visibly affect either PS12, PS14 or PS15 (Fig. 8B). Cuticular specializations in PS14 (spinules on the posterior side of the spiracles in pA8, SO2, SO3 and SO4) and in PS15 (spinules and SO1) appear to be normal.

Uab^1/Uab^1

The spiracles are reduced in Uab^1 homozygotes and SO2 and SO3 are fused (see insert C3, lower left Fig. 8C). SO4 is frequently missing or may be relocated close to the base of SO3. Occasionally, SO1 can be mildly affected. *Uab^1* most severely affects PS14 (pA8/aA9), but leaves PS13 (pA7/aA8) close to normal (Fig. 8C). The group of aA8 spinules just anterior to the posterior spiracles includes normal SO7s, and SO5 and SO6 are likewise present in PS13. Interestingly, some of the specializations in aA7 are affected in a way that suggests transformation of pits and hairs toward sense organs. For instance, leaflets can form in the areas of abdominal hairs h3 and h4, while pegs (see insert C2 in Fig. 8C, upper right) can form in place of a pit. *Uab^1* can apparently cause both losses of function (transformation of PS14 toward 13) and gain of function (transformation of aA7 and other anterior compartments toward aA8). This is characteristic of *r* mutants (D. T. Kuhn and M. Sawyer, unpublished data).

tuh-3/tuh-3

Loss of *tuh-3* function has consequences similar to but less extreme than those of *Uab^1*. The most notable transformations in these larvae are fusion of SO2 and SO3, loss/suppression or translocation of SO4 close to SO3 (see Fig. 6C, D), reduced spiracles, and the occasional gain of function on dorsal aA7 in the form of a group of spinules like those on aA8 (Fig. 7H).

Discussion

Cuticle morphology and segmental organization of the 3rd instar

Our description of 3rd instar cuticles reveals several important differences with the 1st larval stage. These are: (1) loss of hairs on dorsal A1 through A7 by the 2nd instar stage; (2) replacement of the hair sensillum in SO1, SO2, SO4 and SO6 with successively more complex structures in the 2nd and 3rd instars.

The segmental identity of these sense organs and of the tissue surrounding them has been uncertain despite numerous attempts to unravel their origins and relationships. The pattern of *engrailed* expression in this region and the effects of homeotic transformations brought about by several *Abd-B* alleles, confirm that SO5, SO6 and SO7 originate from aA8, that SO2, SO3 and SO4 originate from aA9, and that SO1 originates from aA10. These conclusions are in agreement with the studies of Sato and Denell (1986), and are,

with the exception of the segmental identity of SO4, in agreement with Jürgens (1987). Because the mutant *M3* transforms aA8 and affects SO5, but does not affect SO4, while the mutants *Uab*[1] and *tuh-3* affect aA9 and SO4 but have normal SO5s, our data seem to be most compatible with the suggestion that SO4 derives from aA9 (Sato and Denell, 1986), rather than from aA8 (Jürgens, 1987). Furthermore, *engrailed*-dependent β-galactosidase expression appears to separate SO4 and SO5 into two different regions. Our data additionally complement those of Dambly-Chaudiere and Ghysen (1986) who found SO4 belonging to the A9 sensory neurons.

By following the patterns of *engrailed* expression and examining the phenotypes of *Abd-B* mutants, we have also been able to reconstruct the complex morphological movements that generate the larval caudal segments. Two remarkable conclusions are: (1) that during the process of germ band contraction, pA8 and pA9 cells migrate dorsally so that A10 follows the contracting ventral nervous system to a ventral location below pA8 and A9, and (2) that sometime during embryogenesis the ventral portion of aA8 (posterior side) through aA10 are suppressed. The dorsalization of pA8 and pA9 provides an explanation for the apparent translocation of the anal opening from a position posterior to A9 to a position anterior to A9 between embryonic stages 11 and 12 (for instance, see Fig. 1.1 in Campos-Ortega and Hartenstein, 1985 and Figs 23 and 24 in Turner and Mahowald, 1979). This complex process of rearrangement is intimately linked with the suppression of ventral regions. Almost all structures from the middle of aA8 through aA10 derive from lateral or dorsal structures, and the only structure clearly of ventral origin is the tuft. In A8, for instance, the dorsal surface has an anterior and a posterior component, but only the denticle rows of the anterior compartment are represented on the ventral surface. The remainder of ventral aA8 and pA8, a wide band of naked cuticle accompanied by two rows of anterior pointing denticles, is missing. Furthermore, no posterior compartment *engrailed*-expressing cells can be found between the aA8 denticles and the A10 anal pads. This assumes all *engrailed* expressing cells are posterior and all posterior cells express *engrailed*. Transformations caused by *Abd-B* alleles provide independent support for these conclusions. The missing portion of ventral A8, including the naked cuticle region and anterior pointing denticles at the posterior edge of pA8 is added in the *48* mutant. The *48* mutant transformations also derepress the anterior side of ventral A9, allowing the posterior pointing denticle rows to appear. *Tuh-3* transforms PS14 toward a more anterior segment, and has an expanded band of *engrailed*-expressing cells that extends ventrally from the posterior spiracles to the anterior side of the anal pad. In summary, the only cuticle of ventral origin in segments A8, A9, and A10 is the denticle band of aA8 and the anal tuft.

Three other types of data are consistent with the dorsal/lateral designation for most of the caudal segments. First, spinules blanket all areas of A8-A10 (except for the tuft and anal pad), but in A1-A7 are confined to dorsal and lateral locations. Second, the gain of function phenotype caused by *Uab*[1] and *tuh-3* mutants always results in addition of spinule groups, leaflets and pegs on the dorsal or lateral sides of the 3rd instar larva. No transformations of ventral naked cuticle or pits have been seen in any of these mutants. Third, because *48* transforms all sense organs into abdominal pits and hairs with the appropriate naked cuticle band and spinules accompanying them, even the most ventrally positioned SO1 appears to have derived from dorsal/lateral structures. The caudal segments have been pulled around the posterior end of the embryo at germ band retraction because the pA8 and A9 cells dorsalize, resulting in dorsal/lateral regions taking up ventral locations.

The origin of the anal tuft and the anal pad is uncertain. Jürgens (1987) suggested that the tuft derives from pA11, and the anal pad from aA11. Although our data on *engrailed* expression are consistent with these compartmental designations, our data do not indicate their segmental identity. We favor a pA9 tuft designation, since the *engrailed*-dependent β-galactosidase expression in the tuft is continuous with the pA9 band. However, the tuft is situated between the SO1s which most investigators agree are in aA10. Since it is possible that posterior compartment cells from several segments have fused to make the "A9" posterior compartment, assignment of segmental identity is not straightforward. With regard to the anal pad, we favor the hypothesis that it derives from the anterior side of dorsal/lateral aA10, since *fork head* transforms the anal pad to dorsal/lateral spinules rather than to denticles and posterior compartment staining by *engrailed* is not seen in wild-type embryos or 3rd instar larvae.

The caudal sense organs probably evolved from pits and hairs

Third instar abdominal segments A1 through A7 have a pattern of cuticular specializations that is quite similar. In each segment, dorsal spinules and ventral denticles form a belt that straddles each segment border and virtually encirles the larva. Between these belts are bands of naked cuticle whose cuticular specializations are limited to a characteristic pattern of pits and hairs in each anterior compartment (Fig. 1). However, in segments A8, A9 and A10, no naked cuticle regions exist. Instead, the anterior compartments contain numerous spinules and elaborate sensory cones with pegs and leaflets. Transformations in mutants lacking the function of various homeotic mutants demonstrate that the sensory cones likely derive from the naked cuticle region around and including the pits and hairs. For instance, in *48* homozygotes, PS13 through PS15 are transformed to at least PS12. The transformations are sufficiently complete that the transformed parasegments all have their elaborate sensory cones transformed into pits and hairs. A cluster of a pit-hair-peg is all that remains of SO2 and SO3. Further supporting data come from the mutants *Uab*[1] and *tuh-3* that have partial gain of function phenotypes. These mutants transform pits and hairs in the naked cuticle regions on aA7 and other more anterior segments into groups of spinules characteristic of aA8. Leaflets from SOs replace hairs and occasionally a well formed peg forms in place of a pit. We therefore suggest that the leaflets on the sense organs evolved from abdominal hair sensilla and the pegs evolved from abdominal pits.

Homeotic mutants disrupt parasegments

The *Abd-B* homeotic mutants affect many abdominal segments (Duncan, 1987). We note that this broad domain of function appears to be the consequence of the separate regulation of *Abd-B* in several contiguous parasegmental units: the effects of different partial loss of function alleles we studied most severely affect specific parasegments (reviewed by Martinez-Arias and Lawrence, 1985).

The mutant *M3* primarily affects PS13 (pA7/aA8). Dorsal aA8 is strongly transformed toward aA7 (Fig. 7B). Yet, PS14 (pA8/aA9) appears essentially normal, with the spinule patch on the posterior side of the spiracles completely intact. On the ventral surface of aA8, the transformations include addition of a wide band of naked cuticle lacking the anterior pointing dentical rows at its posterior margin (aA8 does not extend beyond the naked cuticle region). Thus, the ventral transformations stop at the posterior edge of PS13.

Inversion Uab^1 has its most profound loss of function effect in PS14 (pA8/aA9). The posterior spiracles are reduced with the loss of the spinule patch at the posterior spiracle base, and the aA9 SOs are variably affected (Fig. 8C). pA9/aA10 are much less affected, and SO1 is essentially normal (Fig. 8C); the Uab^1 effect in pA7/aA8 is also not strong. The aA8 patch of spinules on the anterior side of the spiracles is normal, as are the aA8 SOs. Addition of ventral denticles anterior to the anal pad shows derepression of pA8 and transformation of PS14 on the ventral surface. However, no wide band of naked cuticle forms between the aA8 denticle band and the pA8 denticles. We interpret this to mean that Uab^1 does not transform PS13 sufficiently to add the naked cuticle band of aA8 back into the pattern. Therefore, the organizational unit controlling segment identity in *M3* and Uab^1 appears to be the parasegment.

The authors thank Drs Welcome Bender and Gines Morata for supplying fly strains. Drs Welcome Bender and David H. Vickers are thanked for many helpful discussions and comments on the manuscript. Support was provided by NSF research grants DMB8811383 and DMB-902393, NATO research grant 930/83, UCF Division of Sponsored Research to D.T.K., NIH research grants to T.B.K. and summer research fellowships to M.S. by ACS, Fla. Div. Inc.

References

Akam, M. (1987). The molecular basis for metameric pattern in the *Drosophila* embryo. *Development* **101**, 1-22.

Boulet, A. M., Lloyd, A. and Sakonju, S. (1991). Molecular definition of the morphogenetic and regulatory functions and the *cis*-regulatory elements of the *Drosophila Abd-B* homeotic gene. *Development* **111**, 393-405.

Campos-Ortega, J. A. and Hartenstein, V. (1985). *The Embryonic Organization of* Drosophila melanogaster. Berlin: Springer-Verlag.

Casanova, J., Sanchez-Herrero, E. and Morata, G. (1986). Identification of a parasegment specific regulatory element of the *Abdominal-B* gene of *Drosophila*. *Cell* **47**, 627-636.

Celniker, S. E., Sharma, S., Keelan, D. J. and Lewis, E. B. (1990). The molecular genetics of the bithorax complex of *Drosophila*: *cis*-regulation in the *Abdominal-B* domain. *EMBO J.* **9**, 4277-4286.

Dambly-Chaudiere, C. and Ghysen, A. (1986). The sense organs in the *Drosophila* larva and their relation to the embryonic pattern of sensory neurons. *Roux's Arch. Dev. Biol.* **195**, 222-228.

Duncan, I. (1987). The bithorax complex. *Ann. Rev. Genet.* **21**, 285-319.

Hama, C., Ali, Z. and Kornberg, T. B. (1990). Region-specific recombination and expression are directed by portions of the *Drosophila engrailed* promoter. *Genes Dev.* **4**, 1079-1093.

Hartenstein, V. (1987). The influence of segmental compartmentalisation on the development of the larval peripheral nervous system in *Drosophila melanogaster*. *Roux's Arch. Dev. Biol.* **196**, 101-112.

Hertweck, H. (1931). Anatomie und Variabilitat des Nervensystems und der Sinnesorgane von *Drosophila melanogaster* Meigen. *Z. Wiss. Zool.* **139**, 559-663.

Janning, W., Labhart, C. and Nothiger, R. (1983). Cell lineage restrictions in the genital disc of *Drosophila* revealed by Minute gynandromorphs. *Roux's Arch. Dev. Biol.* **192**, 337-346.

Jürgens, G. (1987). Segmental organisation of the tail region in the embryo of *Drosophila melanogaster*. *Roux's Arch. Dev. Biol.* **196**, 141-157.

Kankel, D. R., Ferrus, A., Garen, S. H., Harte, P. J. and Lewis, P. E. (1980). The structure and development of the nervous system. In *The Genetics and Biology of* Drosophila, vol 2d (ed. M. Ashburner and T. R. F. Wright). pp. 295-368. London, New York, San Francisco: Academic Press.

Karch, F., Weiffenbach B., Peifer, M., Bender, W., Duncan, I., Celniker, S., Crosby, M. and Lewis, E. B. (1985). The abdominal region of the bithorax complex. *Cell* **43**, 81-96.

Karr, T. L., Weir, M. J., Ali, Z. and Kornberg, T. (1989). Patterns of *engrailed* protein in early *Drosophila* embryos. *Development* **105**, 605-612.

Kiger, J. A. (1976). Cell determination in *Drosophila* with paradoxical genotypes. *Dev. Biol.* **50**, 187-200.

Kuhn, D. T. , Woods, D. F. and Andrew, D. J. (1981). Deletion analysis of the tumorous-head (tuh-3) gene in *Drosophila melanogaster*. *Genetics* **99**, 99-107.

Kuhn, D. T. , Sawyer, M. and Ventimiglia, J. (1992). Cuticle morphology changes with each larval molt in *D. melanogaster*. Dros. Inf. Serv. (in press).

Lewis, E. B. (1978). A gene complex controlling segmentation in *Drosophila melanogaster*. *Nature* **279**, 565-570.

Lindsley, D. J. and Grell, E. L. (1968). Genetic variations of *Drosophila melanogaster*. *Carnegie Inst. Wash. Publ.* No. 627.

Lohs-Schardin, M., Cremer, C. and Nusslein-Volhard, C. (1979). A fate map for the larval epidermis of *Drosophila melanogaster*: localized cuticle defects following irradiation of the blastoderm with an ultraviolet laser microbeam. *Dev. Biol.* **73**, 239-255.

Martinez-Arias, A. and Lawrence, P. A. (1985). Parasegments and compartments in the *Drosophila* embryo. *Nature* **313**, 639-642.

Matsuda, R. (1976). Morphology and evolution of the insect abdomen. Oxford, New York: Pergamon Press.

Nusslein-Volhard, C. (1979). Maternal effect mutations that alter the spatial coordinates of the embryo of *Drosophila melanogaster*. In *Determination of Spatial Organization*, (ed. S. Subtelny and I. R. Kornberg). New York: Academic Press.

Nusslein-Volhard, C. and Wieschaus, E. (1980). Mutations affecting segment number and polarity in *Drosophila*. *Nature* **287**, 795-801.

Patel, N. H., Martin-Blanco, E., Coleman, K. G., Poole, S. J., Ellis, M. C., Kornberg, T. B. and Goodman, C. S. (1989). Expression of *engrailed* proteins in arthropods, annelids and chordates. *Cell* **58**, 955-968.

Sanchez-Herrero, E., Vernos, I., Marco, R. and Morata, G. (1985). Genetic organization of *Drosophila* bithorax complex. *Nature* **313**, 108-113.

Sato, T. and Denell, R. E. (1986). Segmental identity of caudal cuticular features of *Drosophila melanogaster* larvae and its control by the bithorax-complex. *Dev. Biol.* **116**, 78-91.

Tiong, S. Y. K., Bone, L. M. and Whittle, J. R. S. (1985). Recessive lethal mutations within the bithorax-complex in *Drosophila melanogaster*. *Mol. Gen. Genet.* **200**, 335-342.

Turner, F. R. and Mahowald, A. P. (1979). Scanning electron microscopy of *Drosophila melanogaster* embryogenesis. III. Formation of the head and caudal segments. *Dev. Biol.* **68**, 96-109.

Van der Meer, J. (1977). Optical clean and permanent whole mount preparations for phase contrast microscopy of cuticular structures of insect larvae. *Dros. Inf. Serv.* **52**, 160.

Whittle J. R. S., Tiong, S. Y. K. and Sunkel, C. E. (1986). The effect of lethal mutations and deletions within the bithorax complex upon the identity of caudal metameres in the *Drosophila* embryo. *J. Embryol. exp. Morph.* **93**, 153-166.

(Accepted 3 May 1992)

dev8078 4pp colour tip-in

Fig. 5. Embryos stained for engrailed protein and β-gal are shown. (A) Lateral aspect of an engrailed stained embryo at about stage 12. (B) An engrailed-β-gal double stained *ryXho25* embryo showing small pA8 lateral band. (C) A stage-15-16 embryo stained for engrailed protein. (D) A mature stage-17 *ryXho25* embryo stained for β-gal. The embryos are oriented with anterior to the left and dorsal up. ap, anal pad; pA7-pA9, posterior abdominal segments 7 through 9; ps, posterior spiracles; vns, ventral nervous system.

Fig. 7. Nomarski phase interference photomicrographs of β-gal stained en^+ *lacZ tuh-3* and *ryXho25* 3rd instar larvae. (A) Wild-type en^+ staining pattern in caudal 3rd instar segments. (B) Enlargment of A. (C) *tuh-3* larva showing continuous β-gal stain from posterior spiracles to anal pad separating aA8 from aA9. (D) *ryXho25* larva with wild-type β-gal staining where no stain appears between aA8 and the anal pad. Picture oriented as in E. (E) *tuh-3* larva, showing β-gal stain between aA8 denticle band and anal pad (see arrows). (F) *tuh-3* larva showing β-gal stained pA9 and tuft region which does not differ from wild type in D. (G) *tuh-3* larva showing a tiny SO4 (see open arrow) located on the aA9 side of β-gal stained pA8 band. (H) *tuh-3* larva showing gain of function in aA7 and position of stained pA7. Spinule patch around pit p9 of aA7 naked cuticle highlighted with open arrow. aA7-aA9, anterior abdominal segment 7 through 9; AP, anal pad; p8-p9, abdominal pits 8 and 9; pA7-pA9, posterior abdominal segment 7 through 9; PS, posterior spiracles; SO1-SO4, sense organs 1 through 4; SR, stretch receptor; T, tuft.